

Fatigue Mechanisms of Brazed Al-Mn Alloys Used in Heat Exchangers

Aurelien.Buteri^{1,2}, Jean-Yves.Buffière¹, Damien.Fabrègue¹, Elodie.Perrin², Julien.Rethoré³
and Peggy.Havet⁴

¹Universités de Lyon, INSA-Lyon, MATEIS, CNRS UMR 5510, 25 avenue Jean Capelle, 69621
Villeurbanne, FRANCE

²Alcan CRV, Parc Economique Centr'Alp, 725 rue Aristide Bergès – BP27, 38341 Voreppe, FRANCE

³Universités de Lyon, INSA-Lyon LaMCoS, CNRS UMR5259, 18-20 rue des Sciences, 69621
Villeurbanne, FRANCE

⁴Valeo Engine Cooling, 8 rue Louis Lormand, BP 517, 78321 La Verrière, FRANCE

The ratio of aluminum alloys used in the automotive industry tends to increase as a consequence of the enforcement of tougher environmental regulation (minimization of vehicles weight). For example, thanks to their good thermal, corrosion and mechanical properties, aluminum alloys have steadily replaced copper alloys and brass for manufacturing heat exchangers in cars or trucks. Such components have been constantly optimized in terms of exchange surface area and, nowadays, this has led to Al components in heat exchangers with a typical thickness of the order of 0.2 to 1.5 mm. With such small thicknesses, the load levels experienced by heat exchangers components has drastically increased leading to an important research effort in order to improve the resistance to damage development during service life.

This paper focuses on the resistance to fatigue damage of thin sheets of brazed co-rolled aluminum alloys used for manufacturing heat exchangers and particularly on the mechanisms of fatigue cracks initiation. Digital Image Correlation (DIC) has been used to monitor damage development during constant amplitude fatigue tests of thin (0.27 mm) samples. Fatigue cracks have been found to initiate from deformation bands which presence can be correlated with solidification drops at the sample's surface resulting from the brazing process. X-ray tomography has been used to obtain the spatial distribution of drops as well as their characteristics (height, surface...), on the sample gauge length. Those 3D data have been used to produce Finite Element meshes of the samples in order to assess the influence of the drops on fatigue crack initiation.

Keywords: *Fatigue, Al-Mn alloy, X-Ray Tomography, Digital Image Correlation and Finite Elements.*

1. Introduction

The small thicknesses of the thermal heat exchangers components improve the thermal performance through the increase of exchange surface area, but it leads to an increase of the in use loads which can be detrimental to the service life duration via for example fatigue damage development. Fatigue damage of brazed thin sheet aluminum alloys for thermal heat exchangers has rarely been considered in the literature [1 - 4] and none of these works have dealt with thicknesses below 1.5mm.

The main technical issue for the investigation of damage development in fatigue sample with a sub millimeter thickness is that their surfaces cannot be polished. Thus classical optical/electronic microscopy observations of fatigue damage initiation and development cannot be carried out. It has been suggested to use Transmission Electron Microscopy (TEM) to correlate dislocation structures resulting from mechanical cyclic of 3000 series alloy on round gauge section samples with a diameter of 10mm [4]. TEM preparation is however a time consuming and destructive technique. In this study we present a different approach based on DIC [5-6] and 3D tomographic observations.

Those techniques are used to identify fatigue crack initiation sites and perform Finite Element (FE) calculations [7-8], which help to elucidate the fatigue mechanisms of the studied material.

2. Experimental procedure

The present study has been carried out on an industrial material configuration used in heat exchangers. Samples for fatigue tests were made from 3 co-rolled aluminum alloys: a core material (3xxx alloy) and 2 clads (4045 and 7072 alloys). The 3xxx is responsible for the good mechanical properties of the assembly, the 4045 alloy (15% of the thickness) is used as brazing medium for assembling the exchanger's components together and the 7072 alloy (10% of the thickness) improves the internal corrosion resistance. Samples have been manufactured and brazed in industrial conditions to recreate representative microstructures.

2.1 Fatigue tests and digital image correlation

The fatigue test samples investigated had a minimal rectangular section of 4.05 mm^2 ($15 \times 0.27 \text{ mm}^2$) according to the layout of figure 1(a). Fatigue tests were carried out in a hydraulic tension-tension fatigue test machine under stress-amplitude control conditions ($\sigma_{\max} = 100 \text{ MPa}$, stress ratio = 0.1 and $F = 10 \text{ Hz}$) and performed at room temperature. Damage development at the sample surfaces has been monitored during cycling by DIC. A large angle telecentric lens with focal distance of 200 mm associated to a CCD camera with a 1200×1600 pixels resolution ($12 \times 16 \text{ mm}^2$) has been used. Pictures of sample's surface prepared beforehand by applying a speckle are recorded every 150 cycles in constant lighting conditions (exposure time = 15 ms). A Matlab[®] post-treatment [5] of the pictures allows the measurement of the displacement field on the sample surface between two cycling steps and the determination of the equivalent strain and stress fields.

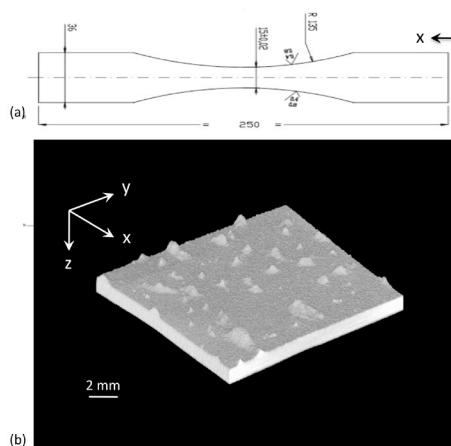


Fig 1: (a): sample geometry. (b): 3D-rendering of the sample surface showing clad solidification drops

2.2 Tomography

X-ray tomography is a (3D) imaging technique basically based on the difference of absorption of the various constituents of the material that allows visualizing the inner structure of an object [9]. This technique has been used here to characterize the surface roughness of fatigue sample.

2.3 Finite element meshing and tensile test simulation parameters

A surface and volume meshing with quadratic tetrahedrons is created from the reconstructed 3D images of the fatigue samples with Amira[®] software. The mesh corresponding to the sample studied here contains 250 000 quadratic tetrahedrons. A Java plugin [7-8] allows to import the mesh into Abaqus[®]. The boundary conditions have been chosen to prevent displacements of sample

extremities except in load direction. Simulation consists in a maximal stress approach in elastic conditions ($E = 70\,000\text{ MPa}$, $\nu = 0.33$) by applying a vertical displacement of 0.1 mm , which correspond to a deformation of 0.2% . The multimaterial aspect of the sample has not been taken into account for the FE calculations.

3. Results and analysis

3.1 Quantitative surface state analysis

A 3D image of fatigue test sample has been obtained by X-ray tomography with a resolution of $13\mu\text{m}/\text{voxel}$. Figure 1(b) shows a part of this sample highlighting the roughness of the surface due to the presence of clad solidification drops (CSD). Those drops are caused by the non-consumption of the liquid clad (4045) into brazed joints during thermal treatment. A quantitative analysis of these surface irregularities can be easily carried out from the 3D data. Figure 2 shows a thickness map of the fatigue sample. It shows that a large deviation from the theoretical thickness before brazing step ($0.27\mu\text{m}$) can be qualitatively appreciated. Quantitative results are exposed in the charts on figures 3(a) and 3(b) for 163 CSD with a minimum volume of 100 voxels ($2.197 \cdot 10^{-5}\text{ mm}^3$). These charts reveal the important correlation between surface and volume of the CSD and their height, which seems to saturate in this material configuration after brazing process.

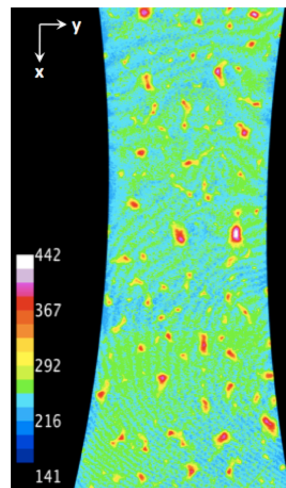


Fig 2: Thickness map of the fatigue test sample from X-ray tomography data (dimensions of the sample: $y_{\text{max}} = 21,5\text{ mm}$ and $x = 45,7\text{ mm}$) – Scale bar in μm

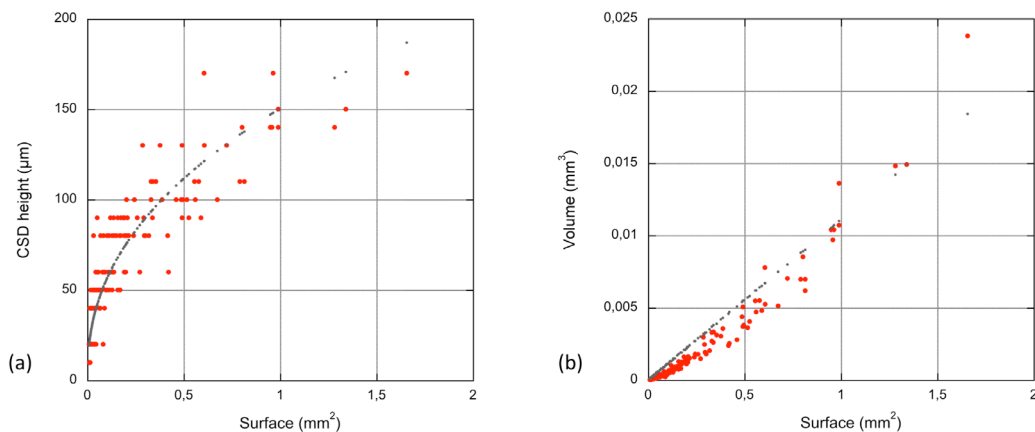


Fig 3: (a): Plot of the clad solidification drops (CSD) height as a function of their surface (dark line: power fit)
(b): Plot of the CSD volume as a function of their surface (dark line: linear fit)

3.2 Fatigue test and digital image correlation

The sample analyzed by X-ray tomography and shown in section 3.1 has been cycled during 933744 fatigue cycles. Test was stopped before fracture (crosshead displacement limit of 130 μm), at this stage sample contained a fatigue crack 1 mm long. Figures 4(a) and 4(b) present the zone of interest (ZOI) used for DIC at reference (750 cycles) and final states. The displacement (U_x) and strain (E_{xx}) fields for 5 specific steps, respectively 47%, 75%, 97% and 100% of the fatigue lifetime, are presented on figures 5 (a-h). Large localized plastic deformation leading to large displacements (figure 5(d)) appears during the last part of the cycling, which probably corresponds to the stable crack propagation. Before the few last cycles (97% of the total number of cycles, i.e. 28 000 cycles), no strain heterogeneity can be visualized by DIC. The presence of a crack can be evidenced by using a discrepancy map (figure 6(c)) as described in [5].

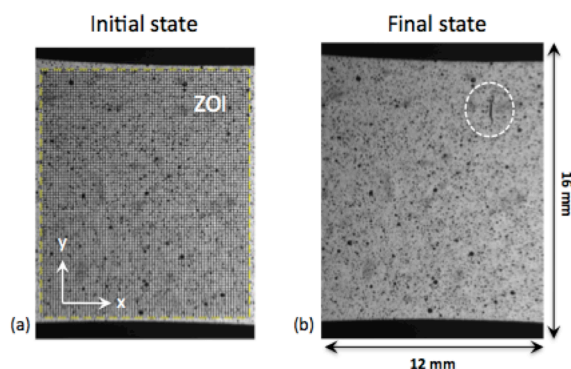


Fig 4: Zone Of Interest (ZOI) for the digital image correlation (DIC) at: (a) the initial state (750 cycles) and (b): the final state (933744 cycles). The painting black points (speckles) are used to calculate displacement field by DIC. Crack can be easily visualized on the final state image (b).

The shadow clearly visible near the crack on figure 4(b) highlights the presence of a CSD. Systematic fractographic analyses of the fatigue samples confirm the presence of a CSD close to the crack initiation zone in most cases. The stress concentration induced by the CSD roughness of the sample surface is likely to promote local plasticity and induce eventually crack initiation. The influence of CSD on local (elastic) stress distribution during cycling can be studied in detail from the 3D FE meshes generated from tomography; this is described in the next section.

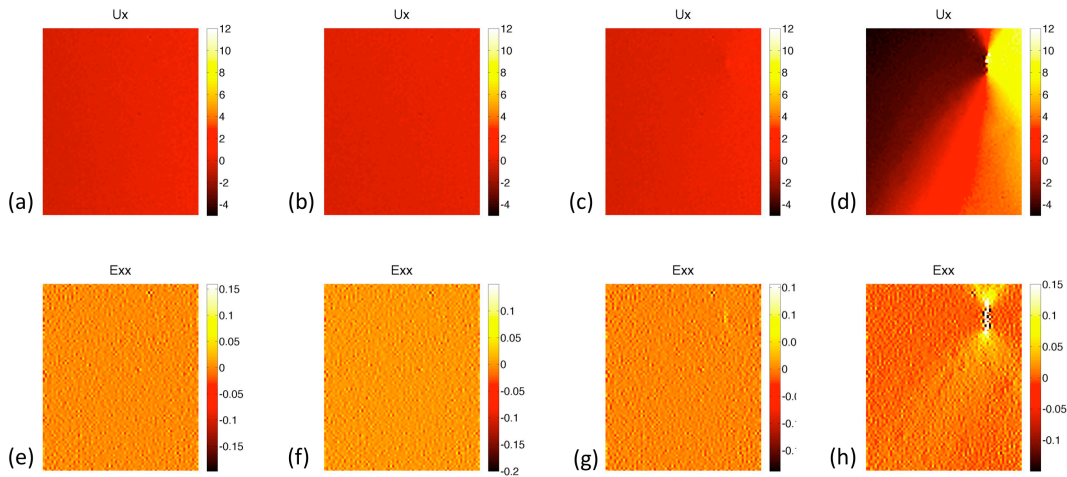


Fig 5: Displacement field U_x (a – d) and strain field E_{xx} (e – h) obtained by DIC at 4 different steps of the fatigue test, respectively 47, 75, 97 and 100% of the lifetime. (Scales - U_x : $\cdot 10\mu\text{m}$ and E_{xx} : $\cdot 100\%$)

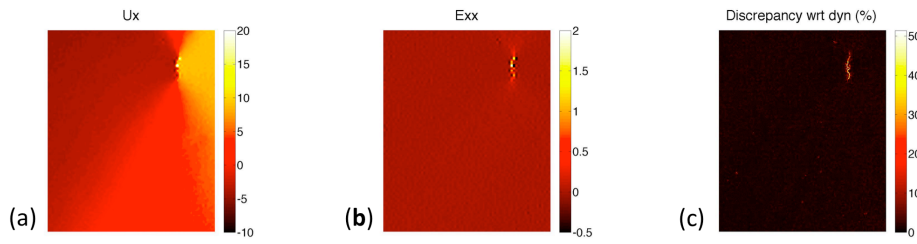


Fig 6: U_x (a), E_{xx} (b) and discrepancy map (c) obtained by DIC at 100% of the lifetime (Scales - U_x : $\cdot 10\mu\text{m}$ and E_{xx} : $\cdot 100\%$)

3.3 Study of clad solidification drops geometric influence by a maximal stress approach

Figure 7 shows the Von Mises stress distribution on the fatigue sample described in the two previous sections. A stress concentration zone can clearly be seen near the different CSDs among which the one responsible for crack initiation. Note that for the model considered here (homogeneous material) the stress concentration zones appear to be localized on the surface.

Moreover, in this case, a parallel between the CSD's height (figure 2) and the important stress concentration induced (figure 7) can be done. Simulation could so appear as an efficient tool to predict crack initiation.

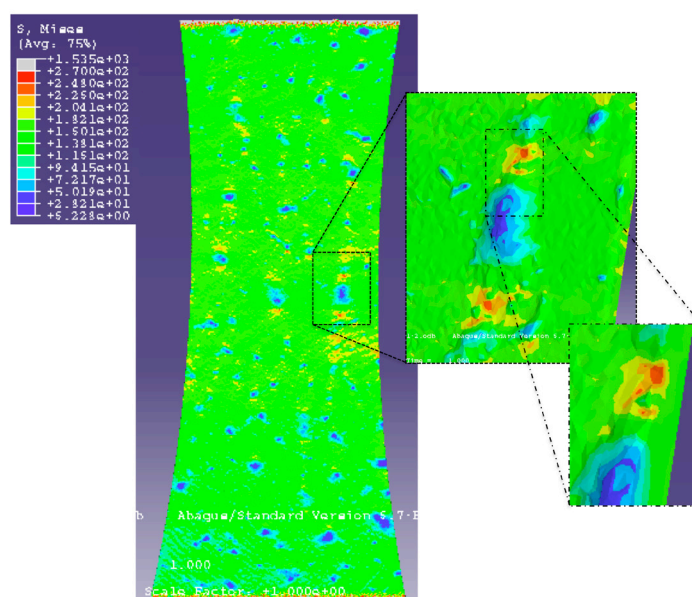


Fig 7: Finite element simulation results of a tensile test on a fatigue sample (elastic calculation). The presence of clad solidification drops clearly induces some stress concentration (Von Mises stresses here). The zoom highlights the CSD responsible for the initiation of the crack shown on figure 4(b).

4. Conclusion

An experimental approach combining digital image correlation, X-ray tomography and microstructurally based finite element calculations has been developed to investigate fatigue mechanisms in thin (0.27mm) fatigue samples of brazed Al-Mn alloys. The results obtained show that the clad solidification drops left on sample's surface after the brazing process induce stress concentrations which can lead to a localization of the plastic strain and to crack initiation. It is worth noticing that 3D X-ray tomography realized on industrial heat exchangers reveals the presence of such clad solidification drops close to fatigue cracks.

A study of the material combining SEM and high resolution Synchrotron X-ray tomography has been performed in order to investigate material microstructure and heterogeneities (intermetallics, Si particles...). The influence of this microstructure on crack location will be studied in the next step and compared to the present results.

Acknowledgments

This work was carried out in the framework of project ELiSE supported by ANR.

References

- [1] X.X.Yao, R.Sandström and T.Stenqvist: Mater. Sci. Eng., A267 (1999) 1-6
- [2] J-K.Kim and D-S.Shim: Int. J. Fatigue. 22 (2000) 611-618
- [3] U.Zerbst, M.Heinemann, C.Dalle Donne and D.Steglich: Eng. Fract. Mech. 76 (2009) 5-43
- [4] H.Yaguchi, H.Mitani, K.Nagano, T.Fujii and M.Kato: Mater. Sci. Eng. A315 (2001) 189-194.
- [5] T.Elgedj, J.Rethoré and A.Buteri: Isogeometric analysis for strain field measurements – in press.
- [6] J.Rethoré, F.Hild and S.Roux: Comput. Meth. Appl. Mech. Eng. 196 (2007) 5016-5030
- [7] J-Y.Buffière, P.Cloetens, W.Ludwig, E.Maire and L.Salvo: M.R.S. Bulletin (2008) 33 – 611-619

- [8] O.Caty, E.Maire, S.Youssef and R.Bouchet: *Acta Mat.* 56 (2008) 19, 5524-5534
- [9] M.Di-Michel, P.Cloetens, L.Salvo and E.Maire: *Techniques de l'ingénieur* (2004) – IN20